

Accepted Manuscript

Influence of annealing temperature on optical properties of zinc oxide thin films analyzed by spectroscopic ellipsometry method

M. Motallebi Aghgonbad , H. Sedghi

PII: S0577-9073(18)30085-6
DOI: [10.1016/j.cjph.2018.04.010](https://doi.org/10.1016/j.cjph.2018.04.010)
Reference: CJPH 506



To appear in: *Chinese Journal of Physics*

Received date: 16 January 2018
Revised date: 21 February 2018
Accepted date: 4 April 2018

Please cite this article as: M. Motallebi Aghgonbad , H. Sedghi , Influence of annealing temperature on optical properties of zinc oxide thin films analyzed by spectroscopic ellipsometry method, *Chinese Journal of Physics* (2018), doi: [10.1016/j.cjph.2018.04.010](https://doi.org/10.1016/j.cjph.2018.04.010)

This is a PDF file of an unedited manuscript that has been accepted for publication. As a service to our customers we are providing this early version of the manuscript. The manuscript will undergo copyediting, typesetting, and review of the resulting proof before it is published in its final form. Please note that during the production process errors may be discovered which could affect the content, and all legal disclaimers that apply to the journal pertain.

Highlights

- Sol-gel spin coating method was used to deposit ZnO thin films.
- The optical properties of the films were determined from ellipsometric data.
- The annealing effect on optical properties of ZnO thin films was studied.
- The single oscillator model was used to find various optical constants.
- Aspnes theory was used to estimate the fraction of voids.

Influence of annealing temperature on optical properties of zinc oxide thin films analyzed by spectroscopic ellipsometry method

M. Motallebi Aghgonbad¹ and H. Sedghi¹

¹ Department of Physics, Faculty of Science, Urmia University, Urmia, Iran

Corresponding author e-mail: m.motallebi89@gmail.com

Zinc oxide (ZnO) thin films were sol-gel spin coated on glass substrates, annealed at various temperatures 300 °C, 400 °C and 500 °C and characterized by spectroscopic ellipsometry method. The optical properties of the films such as transmittance, refractive index, extinction coefficient, dielectric constant and optical band gap energy were determined from ellipsometric data recorded over the spectral range of 300-800 nm. The effect of annealing temperature in air on optical properties of the sol-gel derived ZnO thin films was studied. The transmission values of the annealed films were about 65% within the visible range. The optical band gap of the ZnO thin films were measured between 3.25 eV and 3.45 eV. Also the dispersion parameters such as single oscillator energy and dispersive energy were determined from the transmittance graph using the Wemple and Di Domenico model.

Keywords: Zinc oxide; Sol-gel; Spectroscopic ellipsometry; Annealing temperature

Introduction

Semiconducting devices are mostly based on advancement of thin film technology. Thin film is a two dimensional material deposited by either atom-by-atom or molecule-by-molecule condensation method [1]. ZnO is a unique semiconductor material with a wide band gap of about 3.3 eV [2]. ZnO exhibits many favorable properties, such as high chemical stability, high exciton binding energy of 60 meV, and abundance in nature, and is also regarded as nontoxic [3]. Due to a large free-exciton binding energy, excitonic emission processes can persist at or even above room temperature [4]. Up to now, several methods have been used to fabricate high quality ZnO thin films such as molecular beam epitaxy (MBE) [5], RF magnetron sputtering [6], pulsed laser deposition [7], spray pyrolysis [3,8], chemical vapor deposition (CVD) [9] and sol-gel processing [10]. The sol-gel process is one of the versatile methods to prepare thin film-

supported nano-sized particles without complicated instruments. It is simple, inexpensive, and has a general advantage of large area deposition and uniformity of the films thickness [11]. The properties of the thin films of ZnO fabricated by spin coating technique depend on the deposition parameters such as, precursor concentration, spin speed, pre and post heat treatments. Among these parameters, the post heat treatment is very crucial, because of its role in the modification of crystallinity and surface roughness [12].

Several methods have been used to study the optical properties of ZnO thin films. Among these, SE is a nondestructive method for determining such properties without the limitations of the other methods that have physical contact to the film [13,14]. Ellipsometry method uses detection of polarization state to characterize thin films. Due to dependence of polarization response on structure and optical properties of the films, various informations can be obtained using ellipsometry method [10]. In spectroscopic ellipsometry (SE) method various characterizations including refractive index and dielectric constant are possible. SE has an indirect nature and requires appropriate modeling analysis to extract optical properties. The interpretation of measurement results is rather difficult from the absolute values of (Ψ, Δ) . Thus the construction of optical model is required for data analysis. Ellipsometry data analysis consists of three major parts: dielectric function modeling, construction of an optical model and fitting to measured (Ψ, Δ) spectra. The optical model should be selected according to the optical properties of the sample [15].

In the present work, ZnO thin films were produced by sol-gel spin coating method. The films were subsequently annealed at different annealing temperatures. The optical properties of the annealed films were carried out using spectroscopic ellipsometry (SE) method. Wemple and Di Domenico single oscillator model was used for extracting the dispersion parameters of the films. Effect of annealing temperature on optical properties of ZnO thin films is discussed.

Materials and Methods

The sol solution was prepared by zinc acetate dehydrate as precursor, 2-methoxyethanol as solvent and monoethanolamine as stabilizer. The zinc acetate dehydrate (ZAD) $[\text{Zn}(\text{C}_2\text{H}_3\text{OO})_2 \cdot 2\text{H}_2\text{O}]$ was first dissolved in 2-methoxyethanol ($\text{C}_3\text{H}_8\text{O}_2$) at room temperature. The mixture was stirred by a magnetic stirrer. Monoethanolamine (MEA) ($\text{C}_2\text{H}_7\text{NO}$) was added to the mixture drop by drop until a clear and homogeneous solution formed. The molar ratio of ZAD to MEA was kept 1.0. The concentration of zinc acetate was 0.25 M. The obtained solution

was stirred for 1h at 60 °C. The solution was kept for 24 hours at room temperature for aging and also for optimum viscosity to be obtained. Prior to deposition, the substrates were cleaned in acetone and de-ionized water. ZnO thin films were deposited on glass substrate by spin coating at 4800 rpm. In order to evaporate the solvent and remove organic residuals the films were preheated in air for 10 min at 200°C. Finally, ZnO films were annealed at three different temperatures of 300 °C, 400 °C and 500 °C for one hour. The preheating time of 10 min and the post annealing time of one hour were considered the optimized conditions based on the preliminary investigations.

In this work, the optical analyzing process was done by SE800DUV (SENTECH) spectroscopic ellipsometry instrument with the measurement wavelength range of 300-800 nm, which applies the Step Scan Analyzer measurement mode. Spectra ray software [15] was used for (Ψ, Δ) measurements and fitting process. Measuring optical properties using SE system requires five steps, alignment, ellipsometric measurement, modeling, fitting and reporting. In order to calculate the correct incidence angle and (Ψ, Δ) data, sample height and tilt aligned accurately. Then the incidence angle, the wavelength limit and the polarization position were indicated and the measurement was performed.

When ZnO thin film is formed on glass substrate, the effect of backside reflection leads to complications in the spectroscopic ellipsometry analysis. According to the investigations done by Synowicki [16] to eliminate the backside reflection, in measuring the properties of ZnO thin films, the rear surface of the substrates were roughened and Scotch tape was used during the measurement. In this case, when light enters the Scotch tape, scattering by the cloudy translucent material and backside reflections are suppressed.

Results and Discussion

SE method was used to extract the ellipsometry parameters, psi (ψ) and delta (Δ) which were defined from the ratio of the amplitude reflection coefficient for p and s polarizations [17, 18].

$$\rho \equiv \tan\psi \exp(i\Delta) \equiv \frac{r_p}{r_s} \quad (1)$$

Since in SE method, instruction of an optical model is necessary and the dielectric function of the samples are not known, a model consists of a glass substrate, ZnO thin film, surface roughness layer and air as the ambient medium was designed.

Surface roughness is modeled by a Bruggemann type effective medium approximation (EMA) with 50% of voids and 50% of ZnO. When ZnO thin film is formed on glass substrate, the effect of backside reflection leads to complications in the spectroscopic ellipsometry analysis.

In the modeling step in accordance with the selected material, the proper dispersion formula was used to describe the optical constants dispersion of the thin film. Then the proper model for the sample was made, fit parameters were chosen and the fitting process was done. At last properties such as refractive index, absorption coefficient and dielectric function were calculated.

In this work, Leng-Lorentz oscillator model [19] was used. SENTECH has expanded the formula published by Leng to the following form:

$$\varepsilon(E) = \varepsilon_{\infty} + \sum_{i=1}^N \left(\frac{C_{0i}}{E^2} \left[e^{i\beta_i} (E_{g_i} - E - i\Gamma_i)^{\mu_i} + e^{-i\beta_i} (E_{g_i} + E + i\Gamma_i)^{\mu_i} - 2\operatorname{Re} \left[e^{-i\beta_i} (E_{g_i} + i\Gamma_i)^{\mu_i} \right] - 2i\mu_i E \operatorname{Im} \left[e^{-i\beta_i} (E_{g_i} + i\Gamma_i)^{\mu_i - 1} \right] \right] \right) \quad (2)$$

For a single critical point, C_0 is the amplitude, β is the phase, μ is the order of the pole, E_g is the critical point energy and Γ is the broadening parameter of the oscillator.

In this research we have used a model included a glass substrate, a single film ZnO and a surface roughness on the top of the films. In Fig. 1 the model used in this research is shown.

In Figs. 2 and 3 the experimental and fitted ellipsometry parameters (ψ, Δ), as a function of wavelength for the layers with different annealing temperatures of 300 °C, 400 °C and 500 °C are shown.

To qualify the difference between the experimental and fitted data, the mean square error (MSE) was calculated by following equation:

$$(MSE)\chi^2 = \frac{1}{N} \sum_{i=1}^N \frac{(Mes_i - Th_i)^2}{\sigma_i^2} \quad (3)$$

Where σ_i is the standard deviation of the i -th data point, N is the number of data points, Mes_i is the i -th experimental data point and Th_i is the i -th calculated data point from assumed theoretical model. MSE value obtained by spectroscopic ellipsometry method is shown in table 1.

When the model matches the experimental data as closely as possible, MSE exhibits a minimum value.

In this work, the wavelength limit was chosen 300-800 nm and the polarizer position was selected 45°. The fitting procedure was done in three angles of incidences 60, 65 and 70° (close to the Brewster angle) and the results from analysis of a single angle of incidence 70° are described in detail.

As is mentioned in spectroscopic ellipsometry book written by H. Fujiwara [20], spectroscopic ellipsometry is quite sensitive to surface structures so we should incorporate surface roughness into the optical model in data analysis. By using effective medium approximation (EMA), the refractive index of surface roughness can be calculated. In analyzing surface roughness by EMA, it is required that the morphology of surface roughness be less than $\frac{\lambda}{10}$ of the wavelength.

The films with more surface roughness, lead to decrease in accuracy of analyzing. As, studied in Ref. [12], by increasing annealing temperatures in ZnO thin films, the surface roughness of the films increases. So fitting process in films with higher annealing temperature, should be less accurate, which is also observed in Figs. 2 and 3 and also in the calculated mean square error in table 1.

The transmittance of ZnO thin films deposited on glass substrates with different annealing temperatures is obtained by SE method at normal incidence angle (as is shown in Fig. 4). The transmittance of films is influenced by annealing temperature. In the visible region, all the films have high transmittance. As it can be deduced from Fig. 4, with increasing annealing temperature the thin films became more transparent.

Figs. 5a and b show the wavelength dependence of refractive index and the extinction coefficient of ZnO thin films for different annealing temperatures of 300 °C, 400 °C and 500 °C. In Fig. 5(a) a peak in the wavelength dependence of the index of refraction resulting from the increase in the extinction coefficient at the absorption edge has been observed in ZnO results. As it can be seen for the layers this peak is at 370 nm wavelength. In Fig. 5(b) the extinction coefficient of the layers for different annealing temperatures of 300 °C, 400 °C and 500 °C is shown. It can be observed that for all samples, the extinction coefficient is high at the high ultraviolet region, but the value tends to fall at low visible region. It can be seen that by increasing annealing temperature, the extinction coefficient of the layers increases in the visible wavelength region.

We also calculated the dielectric constant of ZnO thin films. Figs. 6a and b shows the real and imaginary parts of dielectric function respectively for ZnO thin films for different annealing temperatures of 300 °C, 400 °C and 500 °C. It is noted that ϵ_1 and ϵ_2 increase sharply near the optical absorption edge due to the interband direct transition. Here ϵ_2 nearly keeps constant in the visible light range and sharply increases near the optical absorption edge. The behavior of ϵ_1 is similar to refractive index while ϵ_2 mainly depends on the values of extinction coefficient. As it can be seen the values of the real part of dielectric constant is higher than the imaginary part in the visible region.

In Figs. 7a and b the absorption coefficient, α , as a function of wavelength and $\ln(\alpha)$ versus energy of the films are seen respectively for different annealing temperatures. For a given wavelength, the absorption coefficient decreases in the ultraviolet region while increases in visible region. It is known that the absorption coefficient near the band edge shows an exponential dependence on photon energy. This dependence is given as follows [21-23]:

$$\alpha = \alpha_0 \exp\left(\frac{E-E_0}{E_u}\right) \quad (4)$$

Where α_0 , E_0 are constants, E_u is Urbach energy and E is the incident photon energy. The reciprocal of the slope of the linear region in plot of $\ln(\alpha)$ vs. E yields the value of E_u . The absorption edge is known as Urbach edge. The imperfection in the structurally disordered film leads to broadening the bands of localized states. In this case a band gap reduction may occur due to the Urbach edge. Urbach energy is the width of the tails of the localized states associated with the amorphous state in the forbidden band. The optical band gap of thin films can be obtained by Tauc plot [12, 24]:

$$\alpha E = A(E - E_g)^n \quad (5)$$

Where α is the absorption coefficient E is the photon energy, A is an energy-independent constant depending on the electron-hole mobility, having a value between 10^5 (cm)^{-1} and 10^6 (cm)^{-1} [11] and n is 1/2, 2, 3/2 and 3 for allowed direct, allowed indirect, forbidden direct and forbidden indirect band gap semiconductors respectively. For direct band gap semiconductors such as ZnO, $n=1/2$ is selected. The value associated with the intersection point of the straight line region of the plot of $(\alpha E)^2$ versus E with the horizontal axis (E -axis) determined as the band gap E_g , value.

Figs. 8a and b show $(\alpha E)^2$ versus E , and the measured optical band gap energy and Urbach energy of ZnO films for different annealing temperatures. As it can be seen from Fig. 8(b), ZnO thin film with annealing temperature of 400 °C has the highest band gap energy. The slight deviation in the energy band gap from this work compared with the previous work [25-29] may be due to the fact that the values of band gap depend on many factors like coating speed (rpm), the granular structure, the nature and concentration of precursors, the structural defects and the crystal structure of the films.

At room temperature, there are very small numbers of charge carriers that are available in ZnO. The electronically active carriers increase when the temperature increases, thereby leading to an excess carrier in the conduction band. This increase in carriers occurs due to thermal excitation giving rise to the conductivity of the films. The decrease in band gap at annealing temperature of 500 °C may be due to the removal of oxygen vacancies. The removal of oxygen vacancies reduces the carrier density and hence the band gap reduces, which may be attributed to Burstein-Moss shift.

The void fractions of ZnO thin films calculated for the annealing temperatures 300 °C, 400 °C and 500 °C with maple program are shown in Fig. 9 as a function of wavelength. In general, migration of grains should lead to a decrease in fraction of voids. As it can be seen in Fig. 9 ZnO thin film with annealing temperature of 500 °C has the least void fraction.

Wemple and DiDomenico oscillator model can be used to estimate the energy band structures of thin films and to describe the hidden optical origin and mechanism by defining the dispersion energy parameter E_d [30]. This model describes the dielectric response for transitions below the optical gap. In Wemple and DiDomenico model, each electron is considered as an oscillator. This model suggests that within the spectral range of interest, one of the oscillators is considered to be stronger than the rest of the oscillators [12].

The refractive index dispersion can be analyzed by Wemple and DiDomenico single oscillator model. The dispersion data of the refractive index is described as follows [31]:

$$n^2(E) = 1 + \frac{E_0 E_d}{E_0^2 - (\hbar\omega)^2} \quad (6)$$

Where the two parameters E_0 and E_d are connected to optical properties of the thin film and are single oscillator energy and dispersive energy respectively. The values of E_0 and E_d can be

calculated from the intercept and slope of the linear fitted lines by plotting $1/(n^2 - 1)$ versus $(\hbar\omega)^2$ (as shown in Fig. 10). The obtained values of E_0 and E_d are listed in the table 2.

The oscillator energy, E_0 , is an average energy gap. E_0 has an empirical relationship with E_g , which is $E_0 \approx 1.18E_g$ in this work. E_d is a measure of the average strength of the interband optical transitions. The ordering of the film structure leads to E_d increase. From the data obtained, it is shown that the films with annealing temperature of 400°C were more crystalline.

In a single oscillator model, the band gap E_a introduced by Hopfield, provides the link between the single oscillator parameters (E_0, E_d) and the Phillips static dielectric constant parameters ($E_g, \hbar\omega_p$), as follows:

$$E_0 E_a = E_g^2 \quad (7)$$

$$E_a E_d = (\hbar\omega_p)^2 \quad (8)$$

Where, E_g is the optical band gap energy and $\hbar\omega_p$ is the plasma oscillator energy. The calculated values of E_a and $\hbar\omega_p$ are listed in table 2.

Also the refractive index that can be analyzed to obtain the high frequency dielectric constant ϵ_∞ , as follows [32]:

$$\epsilon_1 = n^2 - k^2 = \epsilon_\infty - \left(\frac{e^2}{\pi\epsilon_0 c^2}\right) \left(\frac{N}{m^*}\right) \lambda^2 \quad (9)$$

Where, ϵ_∞ is the high frequency dielectric constant, N is the free charge carrier concentration, ϵ_0 is the permittivity of the free space, e is the charge of electron, c is the velocity of light and m^* is the effective mass of the charge carriers. From the linear dependence of ϵ_1 vs. λ^2 , ϵ_∞ and N can be obtained (as shown in Fig. 11). The relation, $\epsilon_\infty = n_\infty^2$ is used to calculate the long wavelength refractive index. The calculated values of ϵ_∞ , n_∞ and N/m^* are mentioned in table 3.

Conclusion

Zinc oxide thin films have been deposited on glass substrates by sol-gel spin coating method. The films were annealed in the temperatures of 300°C , 400°C and 500°C . Spectroscopic ellipsometry method was used to analyze the optical properties of ZnO films. The transmittance of ZnO thin

films increased with increasing annealing temperature. ZnO thin films with 400 °C annealing temperature had the highest band gap energy and the lowest Urbach energy compared to other films. ZnO thin film with annealing temperature of 500 °C had the least void fraction. The single oscillator model (Wemple and DiDomenico model) was used to find various optical constants such as oscillator energy, dispersion energy, plasma frequency, and carrier concentration. The ordering of the film structure leads to E_d increase. In this work, the films with annealing temperature of 400°C were more crystalline. The film with annealing temperature of 400 °C had the lowest value of carrier concentration.

References

- [1] Mulmi D. D., Dhakal A., and Shah B. R.: 'Effect of annealing on optical properties of zinc oxide thin films prepared by homemade spin coater', *Nepal Journal of Science and Technology*, 2014, 15, (2), pp.111-116
- [2] Jain A., Johari M., Jain A., Pandey P. K., and Agrawal R.: 'Modification in optical properties of ZnO thin film by annealing', *International Journal of Innovative Research in Science, Engineering and Technology*, 2013, 2, (7), pp. 3144-3148
- [3] Nadarajah K., Chee C. Y., and Tan C. Y.: 'Influence of annealing on properties of spray deposited ZnO thin films', *Journal of Nanomaterials*, 2013, 2013, pp.146382 (8 pages)
- [4] Janotti A., and Van de Walle C. G.: 'Fundamentals of zinc oxide as a semiconductor', *Rep. Prog. Phys.*, 2009, 72, pp.126501 (29 pages)
- [5] Darvish D. S., and Atwater H. A.: 'Epitaxial growth of Cu₂O and ZnO/Cu₂O thin films on MgO by plasma-assisted molecular beam epitaxy', *Journal of Crystal Growth*, 2011, 319, pp.39–43
- [6] Hwang Y. H., Kim H. M., Um Y. H., and Park H. Y.: 'Optical properties of post-annealed ZnO:Al thin films studied by spectroscopic ellipsometry', *Materials Research Bulletin*, 2012, 47, pp. 2898–2901
- [7] Vakulov Z. E., Zamburg E. G., Khakhulin D. A., and Ageev O. A.: 'Thermal stability of ZnO thin films fabricated by pulsed laser deposition', *Materials Science in Semiconductor Processing*, 2017, 66, pp.21–25

- [8] Al-zaidi Q. G., Suhail A. M., and Al-azawi W. R.: 'Palladium – doped ZnO thin film hydrogen gas sensor', *Applied Physics Research*, 2011, 3, (1), pp.89 – 99
- [9] Vallejos S., Maggio F. D., Shujah T., and Blackman C.: 'Chemical vapour deposition of gas sensitive metal oxides', *Chemosensors*, 2016, 4, pp. 1-18
- [10] Gilliot M., Hadjadj A., and Stchakovsky M.: 'Spectroscopic ellipsometry data inversion using constrained splines and application to characterization of ZnO with various morphologies', *Applied Surface Science*, 2017, 421, pp.453-459
- [11] Raoufi D., and Raoufi T.: 'The effect of heat treatment on the physical properties of sol–gel derived ZnO thin films', *Applied Surface Science*, 2009, 255, pp.5812–5817
- [12] Chaitra U., Kekuda D., and Rao K. M.: 'Effect of annealing temperature on the evolution of structural, microstructural, and optical properties of spin coated ZnO thin films', *Ceramics International*, 2017, 43, (9), pp.7155-7122
- [13] Uprety P., Junda M. M., Ghimire K., Adhikari D., Grice C. R., and Podraza N. J.: 'Spectroscopic ellipsometry determination of optical and electrical properties of aluminum doped zinc oxide', *Applied Surface Science*, 2017, 421, pp. 852-858.
- [14] Fricke L., Bontgen T., Lorbeer J., Bundesmann C., Schmidt-Grund R., and Grundmanna M.: 'An extended Drude model for the in-situ spectroscopic ellipsometry analysis of ZnO thin layers and surface modifications', *Thin Solid Films*, 2014, 571, pp.437-441.
- [15] Peters S., 'spectra ray and application tutorial, Spectroscopic ellipsometry- theory and application', 2009.
- [16] Synowicki R. A.: 'Suppression of backside reflections from transparent substrates', *Phys. Stat. Sol. (c)*, 2008, 5, pp.1085–1088.
- [17] Gencyilmaz O., Atay F., and Akyüz I., 'Deposition and ellipsometric characterization of transparent conductive Al-doped ZnO for solar cell application', *Journal of Clean Energy Technologies*, 2016, 4, pp.90-94
- [18] Mendoza-Galvan A., Trejo-Cruz C., Lee J., Bhattacharyya D., Metson J., Evans P. J., and Pal U.: 'Effect of metal-ion doping on the optical properties of nanocrystalline ZnO thin films', *Journal of Applied Physics*, 2006, 99, pp.014306 (6 pages)

- [19] Leng J., Opsal J., Chu H., Senko M., and Aspnes D. E.: 'Analytic representations of the dielectric functions of materials for device and structural modeling', *Thin Solid Films*, 1998, 313-314, pp.132-136.
- [20] Fujiwara H.: 'Spectroscopic Ellipsometry Principles and Applications', Published by Maruzen Co. Ltd, Tokyo, Japan, 2007.
- [21] Rajendra B. V., Bhat V., and Kekuda D.: 'Influence of processing parameters on the optical properties of zinc oxide thin films Grown by spray pyrolysis', *International Journal of Emerging Technology and Advanced Engineering*, 2013, 3, (8), pp. 82-85
- [22] Chahmat N., Haddad A., Ain-Souya A., Ganfoudi R., Attaf N., Aida M. S., and Ghers M., 'Effect of Sn doping on the properties of ZnO thin films prepared by spray pyrolysis', *Journal of Modern Physics*, 2012, 3, pp.1781-1785
- [23] Mathew J. P., Varghese G., and Mathew J., 'Effect of post-thermal annealing on the structural and optical properties of ZnO thin films prepared from a polymer precursor', *Chin. Phys. B*, 2012, 21, (7), pp.078104 (8 pages)
- [24] Mahdavi R., and Talesh S. S. A.: 'Sol-gel synthesis, structural and enhanced photocatalytic performance of Al doped ZnO nanoparticles', *Advanced Powder Technology*, 2017, 28, (5), pp. 1418-1425
- [25] Nagarani N., and Vasu V.: 'Structural and optical characterization of ZnO thin films by sol-gel method', *Journal on Photonics and Spintronics*, 2013, 2, (2), pp. 19-22
- [26] Kayani Z. N., Iqbal M., Riaz S., Zia R., and Naseem S.: 'Fabrication and properties of zinc oxide thin film prepared by sol-gel dip coating method', *Materials Science-Poland*, 2015, 33, (3), pp.515-520
- [27] Khan W., Khan Z. A., Saad A. A., Shervani S., Saleem A., and Naqvi A. H.: 'Synthesis and characterization of Al Doped ZnO nanoparticles', *International Journal of Modern Physics: Conference Series*, 2013, 22, pp. 630-636
- [28] Ajadi D. A., Agboola S. M., and Adedokun O.: 'Effect of spin coating speed on some optical properties of ZnO thin films', *Journal of Materials Science and Chemical Engineering*, 2016, 4, pp.1-6

- [29] Khan Z. R., Khan M. S., Zulfequar M., and Khan M. S.: 'Optical and structural properties of ZnO thin films fabricated by sol-gel method', *Materials Sciences and Applications*, 2011, 2, pp. 340-345
- [30] Yong G. X., Chao C., and Sa Z.: 'Optical properties of aluminum-doped zinc oxide films deposited by direct-current pulse magnetron reactive sputtering', *Chin. Phys. B*, 2014, 23, 030701 (1-5).
- [31] Janicek P., Niang K. M., Mistrik J., Palka K., Flewitt A. J.: 'Spectroscopic ellipsometry characterization of ZnO:Sn thin films with various Sn composition deposited by remote-plasma reactive sputtering', *Applied Surface Science*, 2017, 421, pp.557-564.
- [32] Bakry A.: 'Dispersion and fundamental absorption edge analysis of doped a-Si:H thin Films I : p-type', *Egypt. J. Solids*, 2008, 31, (2), pp.191- 204.
- [33] Dalouji V., Solaymani S., Dejam L., Elahi S. M., Rezaee S., and Mehrparvar D.: 'Gap States of ZnO Thin Films by New Methods: Optical Spectroscopy, Optical Conductivity and Optical Dispersion Energy', *Chin. Phys. Lett.*, 2018, 35, 027701 (1-4).
- [34] Komaraiah D., Radha E., Vijayakumar Y., Sivakumar J., Ramana Reddy M. V., and Sayanna R.: 'Optical, Structural and Morphological Properties of Photocatalytic ZnO Thin Films Deposited by Spray Pyrolysis Technique', *Modern Research in Catalysis*, 2016, 5, pp.130-146

Tables

Table 1: Mean square error of ZnO thin films with different annealing temperatures

ZnO thin films	Annealing temp. (°C)	Mean square error
I	300	0.5755
II	400	0.73921
III	500	0.78357

Table 2: The energy of effective dispersion oscillator E_0 , the dispersion energy E_d , the optical band gap E_g , band gap of the single oscillator model E_a , and the plasma oscillator energy $\hbar\omega_p$, of ZnO thin films with different annealing temperatures.

ZnO thin films	Deposition method	Anneal temp (°C)	E_0 (eV)	E_d (eV)	E_g (eV)	$\frac{E_0}{E_g}$	E_a (eV)	$\hbar\omega_p$ (eV)
I	Sol-gel	300	3.93	53.2	3.30	1.19	2.77	12.14
II	Sol-gel	400	4.29	61.3	3.45	1.24	2.77	13.03
III	Sol-gel	500	3.63	40.4	3.25	1.11	2.90	10.82
Ref [12]	Sol-gel	300	4.42	9.22	3.29	-	-	8.84
Ref [12]	Sol-gel	400	4.24	7.72	3.27	-	-	8.19
Ref [12]	Sol-gel	500	3.99	6.09	3.23	-	-	7.33
Ref [33]	RF magnetron sputtering	As-deposited	6.1	58.54	3.21	-	-	-
Ref [33]	RF magnetron sputtering	400	5.8	57.39	3.15	-	-	-
Ref [33]	RF magnetron sputtering	500	5.81	43	3.16	-	-	-
Ref [33]	RF magnetron sputtering	600	5.2	47.37	3.14	-	-	-
Ref [34]	Spray Pyrolysis	As-deposited	6.62	12.49	3.31	-	-	-
Ref [34]	Spray Pyrolysis	450	6.04	12.38	3.26	-	-	-

Table 3: The high frequency dielectric constant ϵ_{∞} , the long wavelength refractive index n_{∞} , and the ratio of free carrier concentration to the free carrier effective mass N/m^* , of ZnO thin films with different annealing temperatures.

ZnO thin films	Anneal Temp. (°C)	ϵ_{∞}	n_{∞}	N/m^* ($\text{kg}^{-1}.\text{m}^{-3}$)
I	300	17	4.12	1.98×10^{56}
II	400	16.8	4.09	1.48×10^{56}
III	500	14.2	3.76	1.81×10^{56}
Ref [12]	300	-	-	4.73×10^{57}
Ref [12]	400	-	-	3.81×10^{57}
Ref [12]	500	-	-	2.75×10^{57}

Figure Captions

Fig. 1 (a) ZnO sample with surface roughness (b) optical model composed of surface roughness and thin film

Fig. 2 The ellipsometry parameter ψ (ψ) extracted by SE method.

Fig. 3 The ellipsometry parameter Δ (Δ) extracted by SE method.

Fig. 4 Transmittance of ZnO thin films for different annealing temperatures of 300 °C, 400 °C and 500 °C.

Fig. 5 (a) the refractive index and (b) the extinction coefficient ZnO thin films with different annealing temperatures of 300 °C, 400 °C and 500 °C

Fig. 6 (a) the real and (b) the imaginary part of dielectric function of ZnO thin films with different annealing temperatures of 300 °C, 400 °C and 500 °C

Fig. 7 (a) the absorption coefficient and (b) $\ln(\alpha)$ versus energy E of ZnO thin films with different annealing temperatures of 300 °C, 400 °C and 500 °C

Fig. 8 (a) $(\alpha E)^2$ versus photon energy E and (b) The measured optical band gap energy and Urbach energy of ZnO thin films with different annealing temperatures of 300 °C, 400 °C and 500 °C

Fig. 9 Fraction of voids of ZnO films with different annealing temperatures as a function of wavelength

Fig. 10 Plot of $1/(n^2-1)$ versus E^2 for ZnO thin films with different annealing temperatures of 300 °C, 400 °C and 500 °C

Fig. 11 Plot of ϵ_1 versus λ^2 for ZnO thin films with different annealing temperatures of 300 °C, 400 °C and 500 °C

Figures

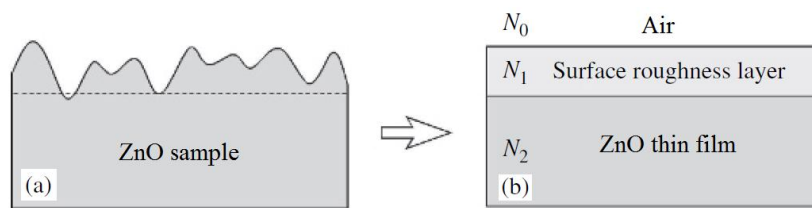


Figure 1

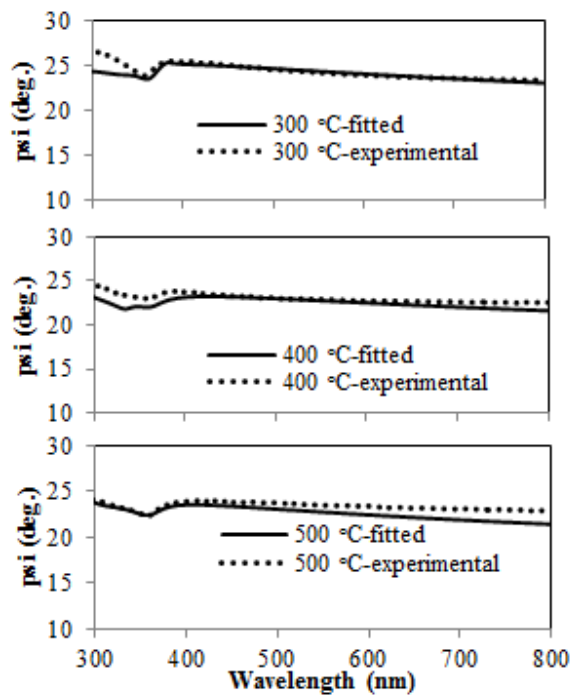


Figure 2

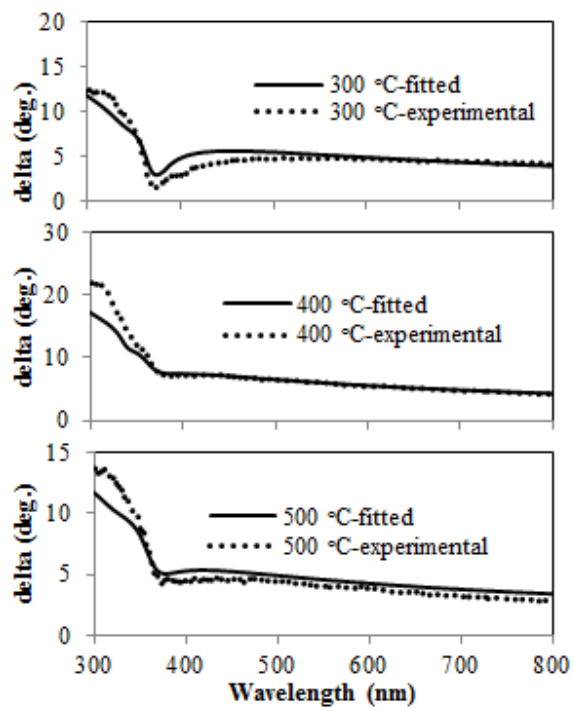


Figure 3

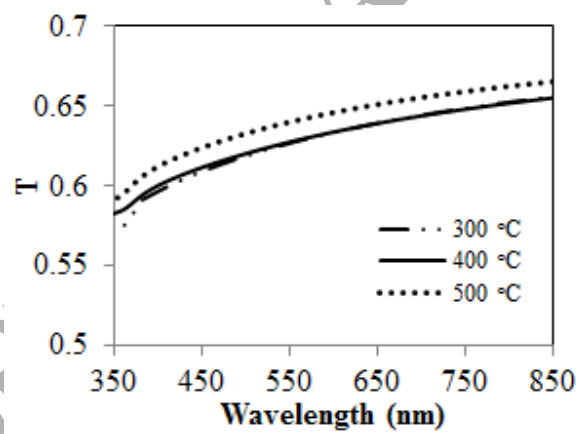


Figure 4

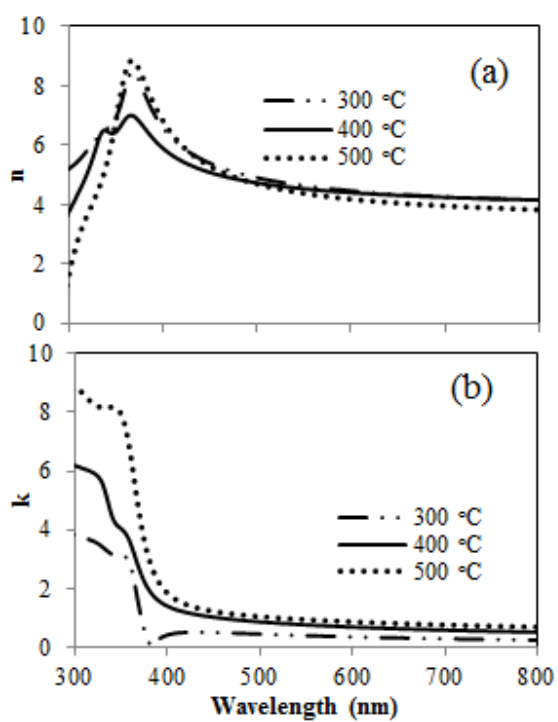


Figure 5

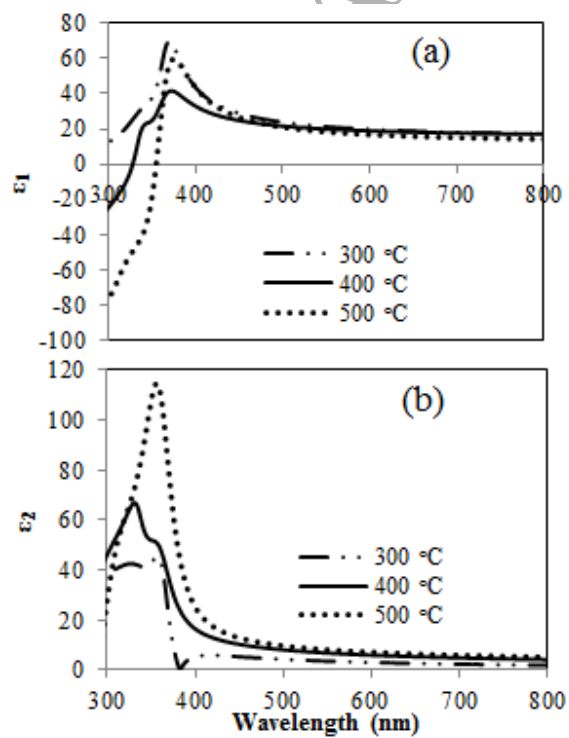


Figure 6

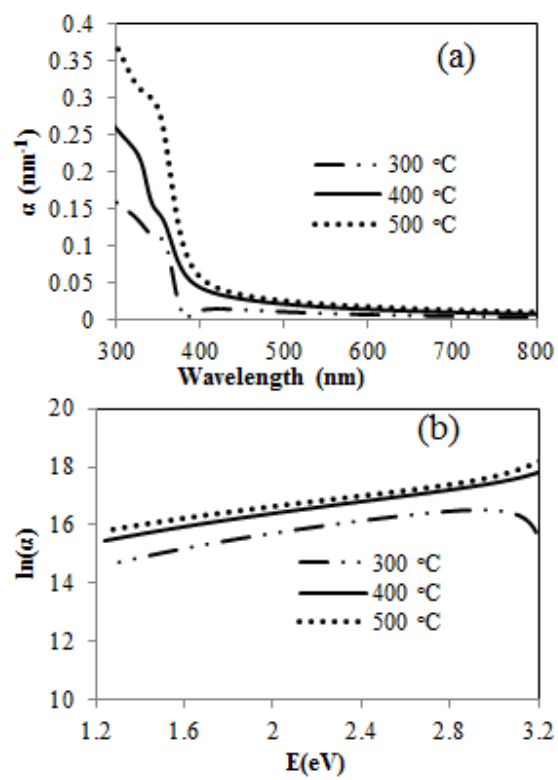


Figure 7

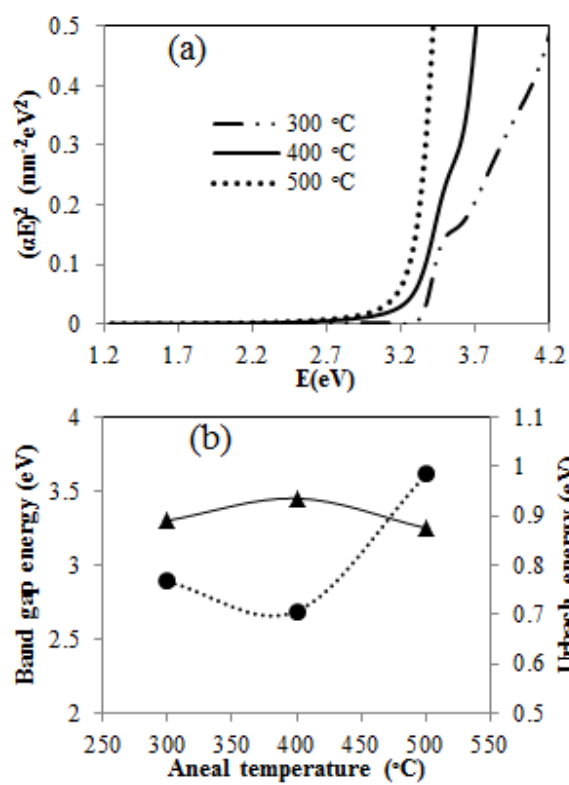


Figure 8

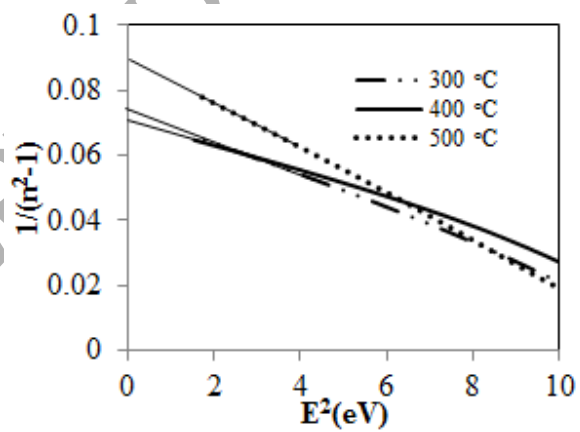


Figure 9

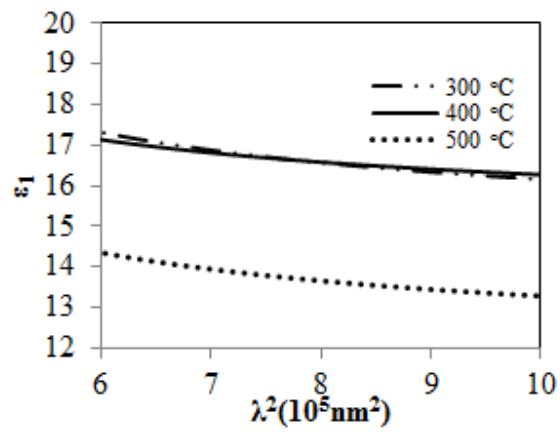


Figure 10

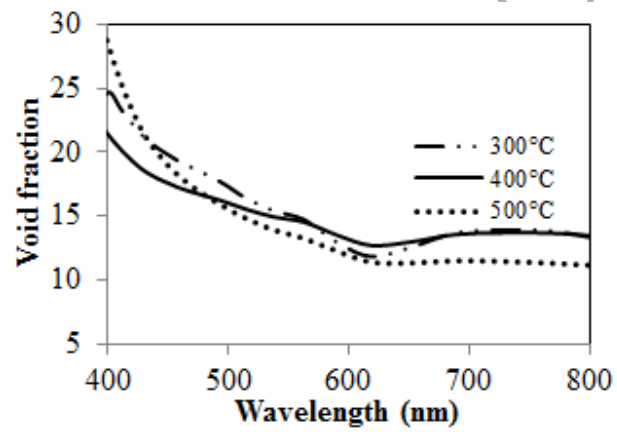


Figure 11